

Petrophysical Characterization of a Clastic Oil Reservoir in the Middle Magdalena Valley Basin in Colombia using Artificial Neural Networks, Seismic Attributes, Well Logs and Rock Physics

¹Ursula Iturrarán-Viveros, ^{2,3}Andrés Muñoz-García, ²Luis Fernando Duque Gómez and ⁴Martin Eduardo Espitia Nery

¹Universidad Nacional Autónoma de México, Ciudad de México, México

²Instituto Tecnológico Metropolitano de Medellín (ITM), Medellín, Colombia

³Departamento de Geociencias, Universidad Nacional de Colombia, Bogotá, Colombia

⁴Departamento de Ingeniería Civil, Universidad Minuto de Dios, Bogotá, Colombia

Key words: ANN, MMVB, parameters, Gamma test, C-Sands

Abstract: We train Artificial Neural Networks (ANN) to estimate the seismic scale of the rock parameters in the lithological units of petroleum interest in Colombia. We apply instantaneous seismic attributes to a stacked P-wave reflected seismic section in the Tenerife field located in the Middle Magdalena Valley Basin (MMVB) in Colombia to estimate effective porosity (ϕ_e), water saturation (S_w), density (ρ) and volume of clay (V_{clay}) at seismic scale. To compute ϕ_e , we use Raymervet equation using the standard parameters for sand formations. The water saturation (S_w) was computed using Simandoux equation for sandstones when clays do not have high cationic interchanges such as in the Tenerife field. The well-logs and the seismic attributes associated to the seismic trace closer to one of the available wells is the information used to train some multi-layered Artificial Neural Networks (ANN). We perform data analysis via the Gamma test, a mathematically non-parametric nonlinear smooth modeling tool, to choose the best input combination of seismic attributes to train an Artificial Neural Network (ANN) for estimating porosity, density, SW and volume of clay. Once the ANN's are trained these are applied to predict these parameters along the seismic line. This is a significant result that shows for the first time a petrophysical characterization of this field at seismic scale. From the continuous estimations of volume of clay we distinguish two facies: sands and shales, these estimations confirm the production of the Mugrosa C-Sands zone and we draw brown clay that correlate with the high amplitude attributes and the yellow sand correlate with the low amplitude attributes.

Corresponding Author:

Ursula Iturrarán-Viveros

Universidad Nacional Autónoma de México, Ciudad de México, México

Page No.: 2728-2733

Volume: 15, Issue 13, 2020

ISSN: 1816-949x

Journal of Engineering and Applied Sciences

Copy Right: Medwell Publications

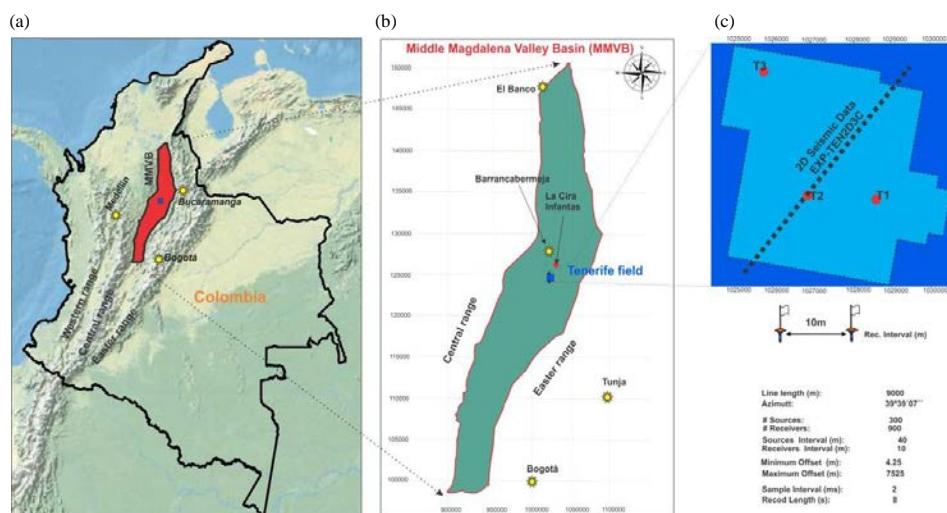


Fig. 1(a-c): (a) Location of the Middle Magdalena Valley Basin (MMVB), (b) Fields La-Cira Infantas and Tenerife and (c) Geometry of the seismic acquisition. Red dots denote the well's locations

INTRODUCTION

Exploration in Sub-Andean basins in Colombia has been traditionally challenging due to the complex geology, rough topography and inaccessible areas. The MMVB is one of the most prolific petroleum basins of Colombia with a long history of hydrocarbon exploration that started with the discovery of a giant oil field called La Cira-Infantas, in 1918. The oilfields in the basin occur mainly as either structural or stratigraphic traps in Tertiary clastic reservoirs. The Tenerife field (Fig. 1), operated by Ecopetrol S.A., is located in the central MMVB, about 20 km South-West of the giant La Cira-Infantas field. This field was discovered in 1971 after positive results of drilling the Tenerife-1 well (T1). The appraisal strategy was followed by the drilling of wells Tenerife-2 (T2) and Tenerife-3 (T3). The development of the field was stopped later due to failed results in T3. T1 and T2 had production of about 100 STBO/day of 22.8 API crude oil, however, they are almost totally depleted today.

ANALYSIS AND INTERPRETATION OF FIELD DATA

We use well log and seismic data from the Tenerife field, in particular, we focus our attention in the 2D-3C P-wave reflected stacked seismic section with an extension of 9 km with 300 sources and 901 receivers. This line crosses the borehole Tenerife-2 which has the following well-log information: Spontaneous Potential (SP), resistivity and induction (ILD), sonic log of P-wave. Some of these logs are more recent such as the Gamma Ray (GR), dipolar sonic logs, check shots and one Offset

Vertical Seismic Profile (OVSP). The well Tenerife-2 has a depth of 7513 ft (Fig. 2), the information available from the core analysis shows that Tenerife-2 crosses some formation units such as Colorado (depth 2462.32 ft), the top of Mugrosa zone (depth 5045.83 ft), the unit Mugrosa B (depth 5004.17 ft) and finally, Esmeraldas formation Zone D (depth 7500 ft approx). An inverse fault crosses Tenerife-2 at depth of approximate 4710 ft. The formation unit Mugrosa C is divided into: Mugrosa C-Sands and Mugrosa C-Shales. The first one has more oil sands, this fact defines Mugrosa C-Sands as the main reservoir of the basin (Fig. 2). It is a sandstone filled with oil, it has a porosity between (20-25%) a water saturation S_w between (40-50%), an oil saturation between (30-40%) and gas saturation between (10-30%) and the approximate permeability is 40.5 cp. With respect to the well Tenerife-2 the zone of Mugrosa C-Sands is located between depths (6857-7255) ft at the top of this formation there are thin layers with depths no >10 ft with high clay content >80%, 10% of sandy clay, pyrite and other minerals. From this top to the bottom we have large sand bodies >100 ft depth with high porosities greater than 15% and small intercalations of clay with small depth widths (5 ft approx). On the other hand, Mugrosa C-Shales defines the bottom of Mugrosa C-Sands, it has a depth of 244 ft, it is made of 80% clay type shale with a porosity <15%; low or null hydrocarbon saturation and very low permeability. The petrophysical model is built based on this information. We compute pseudo-logs for the volume of clay (V_{clay}) using Spontaneous Potential (SP) and the Gamma Ray (GR) well-logs. To compute ϕ_e , we use Raymer equation using the standard parameters for sand formations. The water saturation (S_w) was computed using Simandoux equation for sandstones when clays do

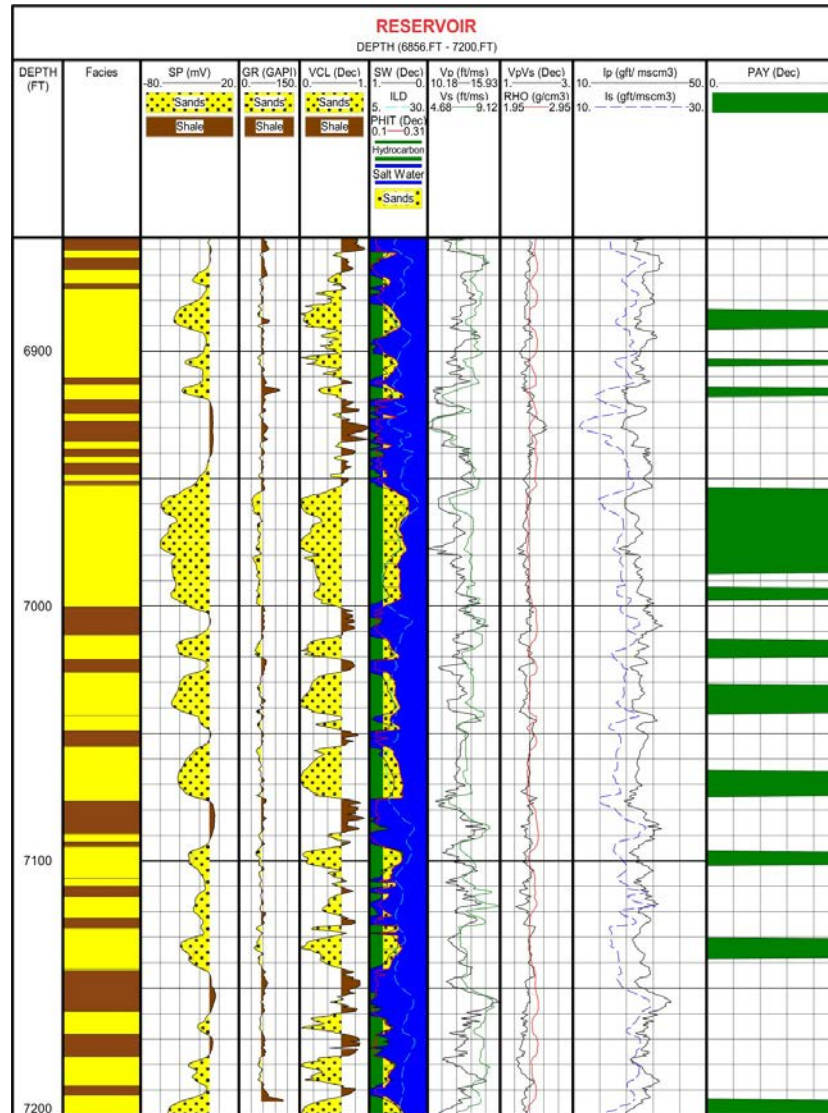


Fig. 2: Well-logs from well Tenerife-2. The eleven paying zones of this well

not have high cationic interchanges such as in the Tenerife field. This methodology is based on Mavko *et al.*^[1] and Donaldson^[2].

NEURAL NETWORK DESIGN AND TRAINING

Our goal is to establish a model to predict ϕ_e , ρ , S_w and V_{clay} logs using a seismic section in the depth interval (2615-7414) ft. that corresponds to the time interval (574-1438 msec). In this interval, we have well-log information from the borehole Tenerife-2 as the training data set. We follow the same approach given by Parra *et al.*^[3], Iturraran-Viveros and Parra^[4], Iturraran-Viveros^[5] and perform the Gamma test analysis, Jones^[6] to select the best combination of inputs to train an ANN. This is a critical step to devise a systematic feature

selection scheme that provides guidance on choosing the most representative features for estimation of petrophysical parameters. We take the definitions of seismic attributes given by Taner *et al.*^[7], Taner^[8], Chopra and Marfurt^[9] and Barnes^[10] and we start with a collection of 19 seismic attributes (including time): time = t , seismic trace = $s(t)$, variance = σ_t^2 , attenuation, sweetness, RMS amplitude = $ARMS(t)$, inst. bandwidth = ωB , Local structural azimuth, local flatness, iso-frequency, Dip illumination, dip deviation, chaos, amplitude, edge detection, envelope, edge evidence (from amplitude contrast), AVO and first derivative = $ds(t)/dt$. According to the Gamma test for this data set the best combination of attributes to estimate S_w is: $s(t)$, σ_t^2 , $A(t)$, ω , envelope, edge evidence and $ds(t)$. On Fig. 3, we can see the final estimations at seismic scale of

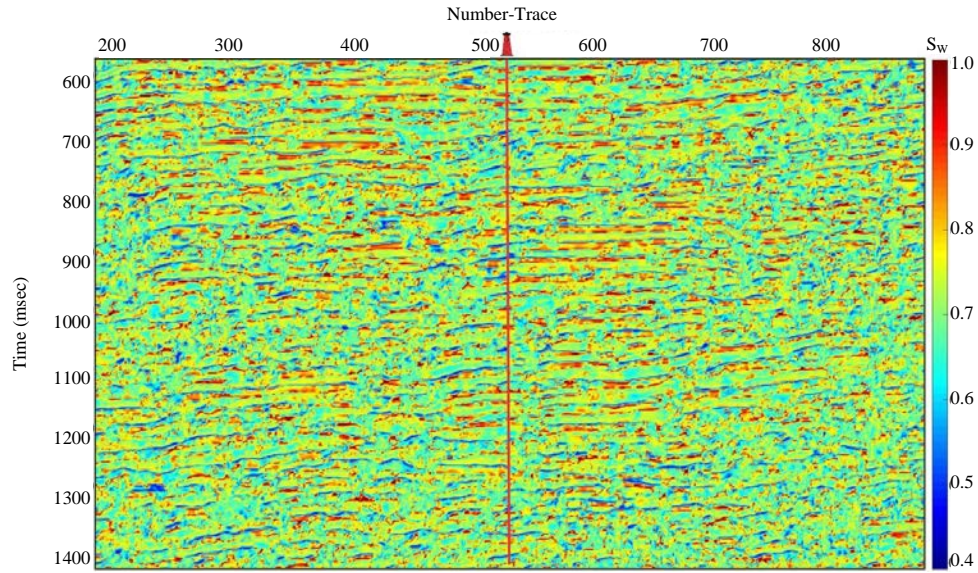


Fig. 3: Estimation of S_w at seismic scale

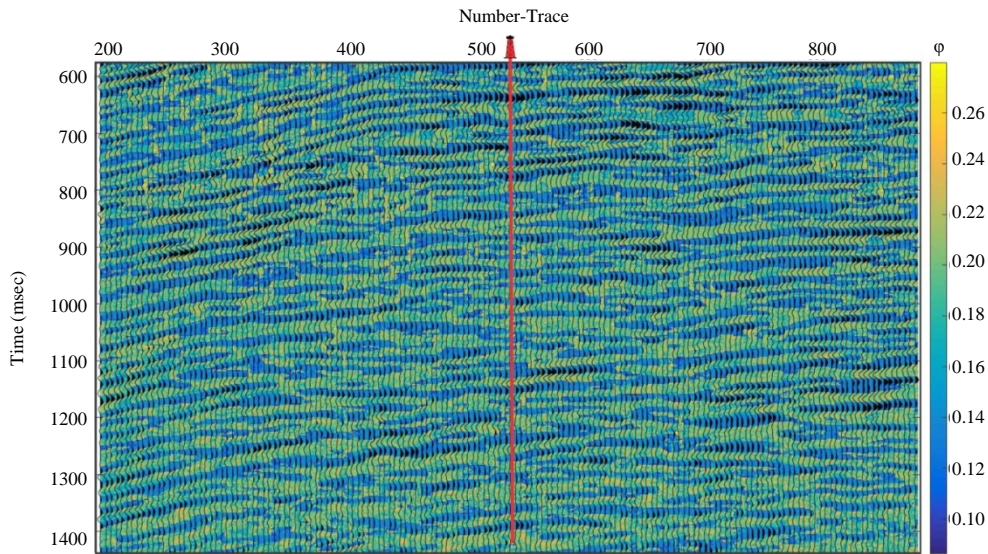


Fig. 4: Estimation of effective porosity at seismic scale

S_w obtained by the trained ANN. To estimate ϕ , we use: t , $s(t)$, dt , σ_t^2 , $A(t)$, ω , envelope, edge evidence and $ds(t)$, on Fig. 4, we have the final estimations at seismic scale of ϕ obtained by the trained ANN.

To estimate ρ the Gamma test indicates that the best combination of attributes is: t , $s(t)$, sweetness, Local structural azimuth, local flatness, dip illumination, dip deviation, chaos, amplitude, edge detection, envelope, edge evidence (from amplitude contrast), AVO and first derivative = $ds(t)/dt$. Finally, to estimate V_{clay} , we used: $s(t)$, attenuation, sweetness, ωB , local structural azimuth,

iso-frequency, Dip deviation, Chaos and $ds(t)$. Using dt the most suitable combination of attributes for each petrophysical parameter, we have trained using three different algorithms of supervised multi-layered Artificial Neural Networks: Backpropagation, Broyden-Fletcher-Goldfarb-Shanno (BFGS) and Conjugate Gradient. The best results obtained for r were using a BFGS with 14 inputs, two hidden layers of 8 neurons each and one output (14-8-8-1). In order to estimate ϕ_e , we used a backpropagation ANN with 8 inputs, two hidden layers of 10 neurons each and one

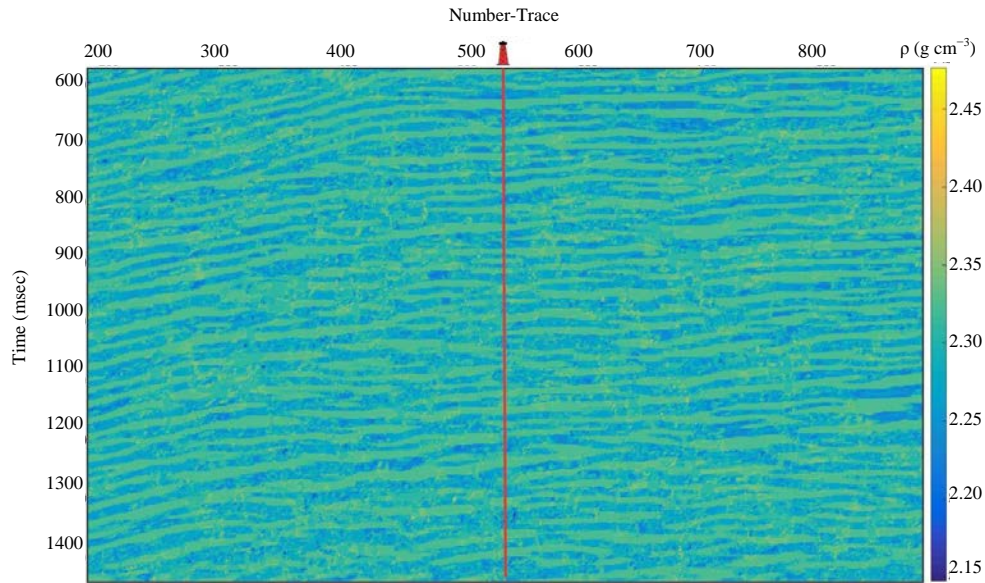


Fig. 5: Estimation of ρ at seismic scale

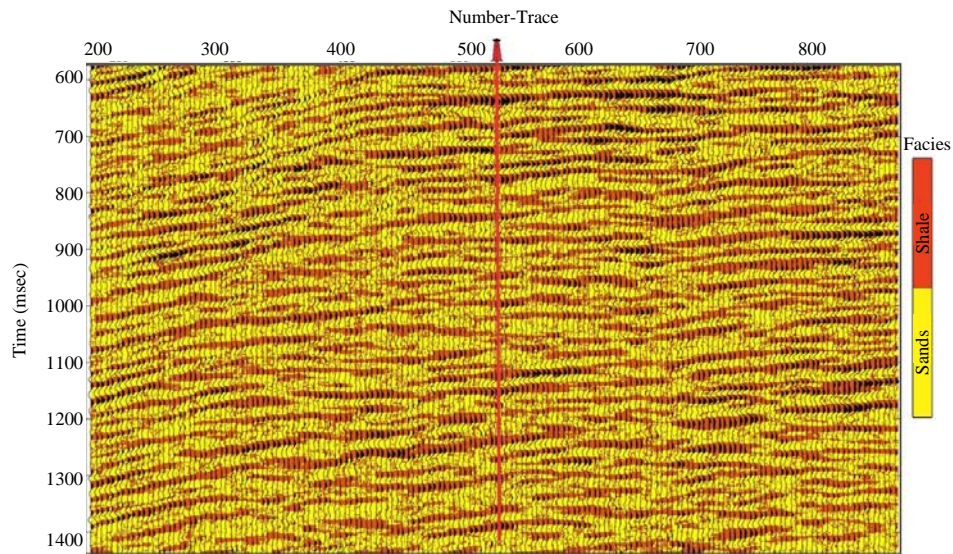


Fig. 6: Facies (sands in yellow, shales in brown) at seismic scale obtained from the estimation of V_{clay}

output (8-10-10-1), S_w with a (9-10-10-1) BFGS ANN and V_{clay} using a (10-10-10-1) Conjugate Gradient ANN.

We have trained the ANN and test its capability of generalization using a testing/validation data set (20% of the original data set) which was not known for the ANN and the agreement was very satisfactory. Once the ANN show the capability of generalization we feed the trained ANN with the 901 seismic traces that correspond to the area of interest close to the the borehole Tenerife-2. The estimations obtained at seismic scale using these ANN for ϕ_c are shown in Fig. 4. Figure 5 shows the estimations of

ρ at seismic scale. The well used for this study Tenerife-2 is located in the middle of the section. The high estimations of porosities in Fig. 4 are in red and low porosities are in green, the same for S_w in Fig. 3 high saturation are in red and low water saturations are in green. When estimating the V_{clay} , we observed that the layered structure was very distinctive, so, we decided to establish a facies characterization by assigning class 1 = sand to the values of $V_{\text{clay}} < 0.5$ and class 2 = shale to those values that satisfy $V_{\text{clay}} \geq 0.5$. Figure 6 shows the result of this facies classification. Some brown clay correlate with the high amplitude attributes and the yellow

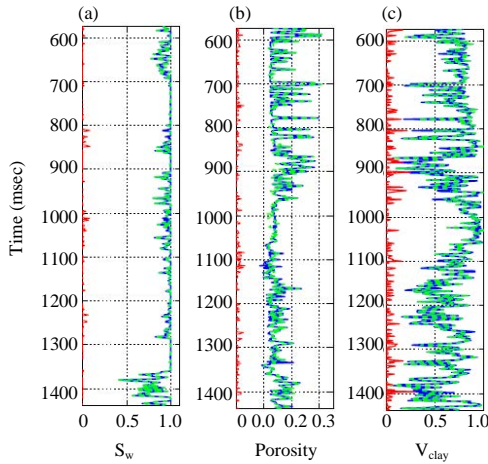


Fig. 7(a-c): Well-log information in each track S_w , ϕ_e , V_{clay} in blue lines, green lines represent the ANN estimations and in red the absolute error

sand correlate with the low amplitude attributes. The higher amplitude attributes are small reflectors that are caused by the change on the impedance contrast between the brown clays and the yellow sands. The brown clays are stiffer (compact material of low porosity). On the other hand the yellow sands are softer and probably with some degree of porosity. Since, the yellow clay is associated with dispersive waves, this suggests high attenuation. One possible interpretation is that the yellow clay unit has a laminated structure that can produce the waves to be dispersive and broaden (this is called scattering attenuation effects). The soft brown clays with yellow clays are part of a laminated structures as well. There might be two types of brown shales, some are more stiff than others. The least stiff brown clays and the yellow clays form the laminated structures (Fig. 7).

CONCLUSION

The facies estimated here at seismic scale agree with the sand bodies and its small clay intercalations identified by the well-logs. The results far away from the borehole also allow to identify continuous sand bodies with shally intercalations and in many cases it is possible to distinguish between the limits of the sand zone. On the other hand the results for ϕ_e and S_w in the well

neighborhood are in agreement with core analysis and well-log information. We observe a good correlation with the amplitudes of the seismic data.

ACKNOWLEDGEMENTS

We thank Ecopetrol S.A. within the research program 0266-2013 Colciencias Ecopetrol, for providing the well and seismic data used in this research. This work was partially supported by CONACYT México under PROINNOVA projects 241763, 231476 and DGAPA-UNAM project number IN100917.

REFERENCES

01. Mavko, G., T. Mukerji and J.P. Dvorkin, 2009. The Rock Physics Handbook. 2nd Edn., Cambridge University Press, UK.
02. Tiab, D. and E.C. Donaldson, 2004. Petrophysics. 2nd Edn., Elsevier, New York, USA.,.
03. Parra, J.O., U. Iturraran-Viveros, J.S. Parra and P.C. Xu, 2015. Attenuation and velocity estimation using rock physics and neural network methods for calibrating reflection seismograms. Interpretation, 3: SA121-SA133.
04. Iturraran-Viveros, U. and J.O. Parra, 2014. Artificial neural networks applied to estimate permeability, porosity and intrinsic attenuation using seismic attributes and well-log data. J. Applied Geophys., 107: 45-54.
05. Iturraran-Viveros, U., 2012. Smooth regression to estimate effective porosity using seismic attributes. J. Applied Geophys., 76: 1-12.
06. Jones, A.J., 2004. New tools in non-linear modelling and prediction. Comput. Manage. Sci., 1: 109-149.
07. Taner, M.T., J.S. Schuelke, R. O'Doherty and E. Baysal, 1997. Seismic trace attributes and their projected use in prediction of rocks properties and seismic facies. Technical Report, Rock Solid Images, Inc., Houston, Texas.
08. Taner, M., 2001. Attributes revisited: Technical report. Rock Solid Images, Inc., Houston, Texas.
09. Chopra, S. and K.J. Marfurt, 2007. Seismic Attributes for Prospect Identification and Reservoir Characterization (Geophysical Developments Series 11). Society of Exploration Geophysicists, USA.
10. Barnes, A.E., 2015. Handbook of Post-Stack Seismic Attributes. Society of Exploration Geophysicists, Tulsa, Oklahoma.,.